IMEKO International Conference on
Metrology for Archaeology and Cultural Heritage
Lecce, Italy, October 23-25, 2017

Experimental and numerical analysis on masonry arch built with fictile tubules bricks.

Renato S. Olivito[1], Carmelo Scuro[1], Rosamaria Codispoti[1]

[1] *Department of Civil Engineering, University of Calabria, Via Ponte P. Bucci (cubo 39B), 87036 Rende (CS), ITALY*
{renato.olivito, carmelo.scuro, rosamaria.codispoti}@unical.it

***Abstract* – Numerous archaeological discoveries made all over the Mediterranean area have highlighted the use of a particular building technique based on fictile tubules bricks. This building technique was commonly used for the building of walls and domes in thermal baths and masonry kilns since the Roman Empire. This paper investigates the behavior of structures employing such technology via experimental tests and numerical analysis. In order to obtain the value of force that induced in the structure the develop of the first cracks, a masonry scale arch was built and tested in the laboratory of University of Calabria. After that, numerical and analytical models were performed to verify and validate the experimental results obtained. The numerical models were created using the software COMSOL.**

I. INTRODUCTION

Fictile tubules are cylindrical clay bricks with a hollow conformation that provides thermal insulation and ensures lightness in the structural elements. This well serves the purposes of thermae and kilns, since heat dispersion affects their functionality. Fictile tubules were usually either embedded in mortar in staggered manner or assembled with a female-male coupling system. [1]

These constructive elements are identified such as the first hollow bricks of the history and they assumed different sizes and shapes in according to the geographic areas where they were made [2]. During the research of sites characterized by construction made with fictile tubules carried out in the area of Mediterranean, it was possible identify three different types of these particular bricks: the amphorae, fictile tubules and caroselli. All types of fictile tubules were made by the potter that used the clay as raw material. The different clay used, that changed in according to the geographic area, assigned at these elements different colors and mechanical strength. This diversification depends on the mineralogical composition of the clay and the presence of iron oxide and calcium oxide inside them [2].

Fictile tubules are characterized by a syringe shape with the tip being a truncated cone. During the construction phase, the tip itself was inserted into the next element – characterized by a perforated base – thus ensuring the interlocking with each other. The structures with this technique was made by juxtaposition of arches (Fig. 1.a).

The amphorae were characterized by shapes similar to those employed for creating the ceramic vessels of the same name. They were positioned inside the structure before casting a cement conglomerate jet to ensure the formation of voids and consequently decreasing of the stress (Fig. 1.b).

The technique used to make the scale model is that with caroselli. It differs from the other because it uses a radial and staggered arrangement of the elements over a centering and is completed with a cement conglomerate jet. [3]

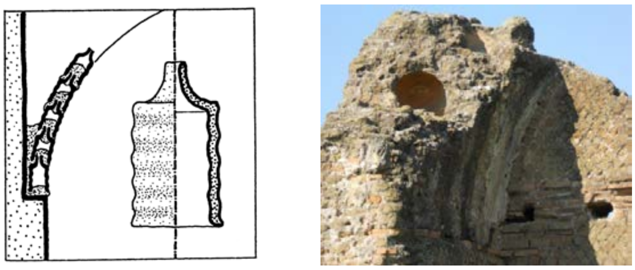

a) b)

Fig 1. a) Barrel vault made with fictile tubules [4] b) amphora in Villa delle Vignacce

II. EXPERIMENTAL TEST

The masonry arch used for the experimental campaign has an internal span equal to 1500 mm, a width of 500 mm and a thickness of 150 mm (Fig. 4a). Caroselli are arranged in a staggered manner, with their circular base tangent to the intrados. Mortar joints of approximately 20 mm separate each row of elements. The arch was built using a wooden centring and two concrete blocks. The blocks were fixed to the ground for supports and connected with two steel beams. After the arch was completed, a final cast of mortar, of about 30 mm, was placed on it. The wooden centring was carefully removed after thirty days. [5]

Fig.2 Set up of static test

The static test was conducted using a manual hydraulic load cell. The load was applied to a steel beam welded to a cylindrical element, aligned to the keystone section (Fig. 2). Four displacement transducers were used to measure vertical displacement of the arch (Fig. 3). The test was stopped when the first cracks were occurred in the structure. The maximum value of the force recording during the test was equal to 6.4 kN.

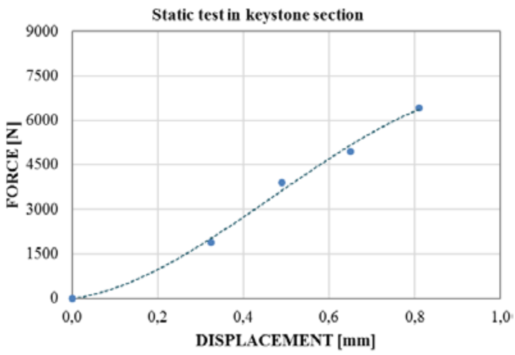

Fig.3 Maximum load-displacement diagrams in the keystone section

III. ANALITICAL MODEL

In order to obtain a validation of static tests conducted on the scale model, an analytical verification was carried out by solving an isostatic arch scheme characterized by a concentrated load located in keystone. The equivalent isostatic scheme used is the three-hinge arch. Two steel beams were fixed to the blocks of concrete at the base of the arch with a single bolt, in order to prevent displacement during the test. This condition was assumed in the analytical model with the presence of two hinges. Instead, the non-perfect adhesion between mortar and fictile tubules in keystone caused a rotation due to the load, as shown in the Figure 4. The latter Figure show how the cracks develop inside the mortar without affecting the fictile tubules suggesting the analysis of the section composed only of mortar.

Fig.4 Crack in keystone during the test.

The isostatic scheme was solved by imposing the value of the concentrated load equal to first cracking load, achieved experimentally. The values of the internal reactions obtained and the normal stress, shear stress and bending moment diagrams were calculated and show in Figure 5.

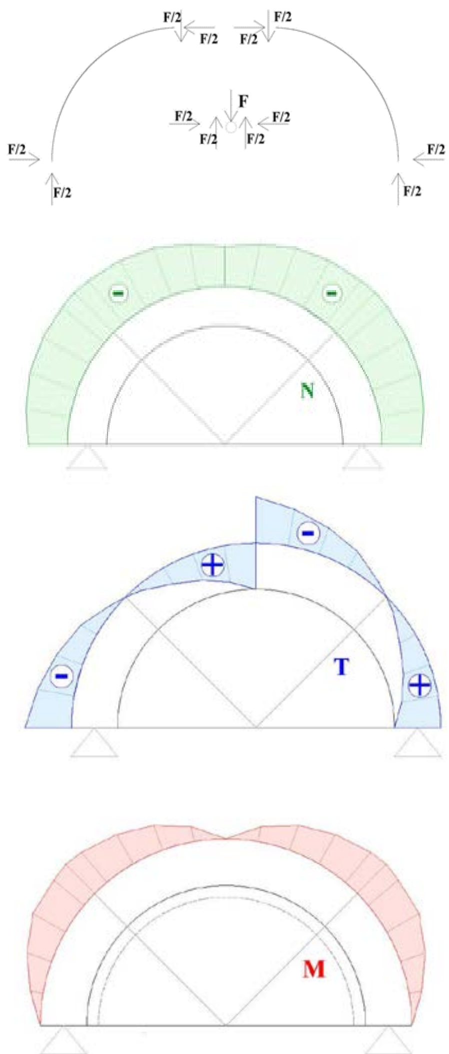

Fig.5 Internal reactions and diagrams of normal stress (N), shear stress (T) and bending moment (M)

The analytical study performed in the section at 45 ° shown that both the bending moment and the normal stress assumed maximum values. This cross section, composed by only mortar, coincides with the part of the arch where the first crack appeared during the static test and it was investigated as a section subject to great eccentricity with the following equations:

$$I_n = S_n \cdot d_n \tag{1}$$

$$I_n = \frac{b \cdot x_c^3}{3} + \frac{n_{ct} \cdot b(h - x_c)^3}{3} \tag{2}$$

$$S_n = \frac{b \cdot x_c^2}{2} + \frac{n_{ct} \cdot b(h - x_c)^2}{2} \tag{3}$$

$$d_n = e - \frac{h}{2} + x_c \tag{4}$$

The equations [1-4] are used in order to obtain the value of neutral axis x_c, that is equal to 70,75 mm.

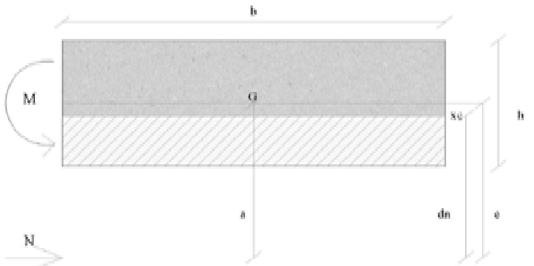

Fig.6 Cross Section investigated

The value of the bending moment, that caused the develop of the first cracks in the extrados of the section at 45°, is evaluated with the equation 5.

$$M_{ct} = \frac{\sigma_t \cdot I_n}{n_{ct} \cdot (h - x_c)} \tag{5}$$

From the value of M_{ct}, it is easy to obtain the value of the load (F) with equation 6.

$$F = \frac{2 \cdot M_{ct}}{r \cdot (Sen(\alpha) + Cos(\alpha) - 1)} \tag{6}$$

the Load (F), analytically estimated, is equal to 6252 N, and it is 200 N lower than that obtained experimentally.

IV. NUMERICAL MODEL

From the tests carried out in the laboratory on the masonry arch, it was found that the crack was developed along the section made up of only mortar, without affecting the fictile tubules. In addition, the applied force has induced the formation of the first crack on the left side, suggesting to create a numerical model with a reduction in mechanical properties in the same cross-section of the structure. The develop of the damage in the section, composed of only mortar, has induced to create a numerical model characterized by perfect adhesion between the mortar and fictile elements. In order to predict the develop of the crack, Mazars Damage Model was implemented in the software COMSOL [6].

Mazars in 1984 proposed a isotropic damage model to concrete, based on two scalar variables of damage that were independent, linked to tensile stress and compressive strength. This model was based on: the possibility of evolution of mechanical properties after a damage threshold, different tensile and compression behavior, and the fact that the damage could be permanent in the material.

The formulation is based on the isotropy hypothesis of the material, which for masonry walls is not valid. However, the difficulty of having a reliable experimental characterization of such anisotropy makes acceptable the approximation that can be obtained by using isotropic models. [7]

The model introduces two independent scalar variables *Dt* and *Dc*, respectively used when the stress is positive or negative.

In a multi-axial stress state, the positive and negative stress are distinguished by dividing the stress tensor in according to the sign of the principal stress:

$$\sigma = \sigma_+ - \sigma_- \tag{7}$$

The matrix may be written as:

$$\sigma = \begin{bmatrix} \sigma_1 & 0 & 0 \\ 0 & \sigma_2 & 0 \\ 0 & 0 & \sigma_3 \end{bmatrix} = \begin{bmatrix} \langle\sigma_1\rangle & 0 & 0 \\ 0 & \langle\sigma_2\rangle & 0 \\ 0 & 0 & \langle\sigma_3\rangle \end{bmatrix} - \begin{bmatrix} \langle-\sigma_1\rangle & 0 & 0 \\ 0 & \langle-\sigma_2\rangle & 0 \\ 0 & 0 & \langle-\sigma_3\rangle \end{bmatrix}$$

where diagonal components are processed by Mc Auley function.

The constitutive law of the strain is:

$$\begin{aligned} \varepsilon = {} & \frac{1}{E_0(1-D_t)}\left[(1+\nu_0)\cdot\sigma_+ - \nu_0\langle tr\sigma\rangle_+ \cdot I\right] + \\ & + \frac{1}{E_0(1-D_c)}\left[(1+\nu_0)\cdot\sigma_- - \nu_0\langle tr\sigma\rangle_- \cdot I\right] \end{aligned} \tag{8}$$

E_0 and v_0 are the Young module and the Poisson coefficient respectively, while *I* is the second order identity tensor. In this model the two damage variables *Dt* and *Dc* have two evolutions different and independent of each other. For example, the damage due to tensile stress does not influence the compression. [7]

In a multi-axial state, the strain tensor is split into a positive part and a negative part depending on the sign of the main strain, similarly to what was done by Mazars for the stress tensor (Eq. 9)

$$\varepsilon = \varepsilon_{+} - \varepsilon_{-} \tag{9}$$

The matrix may be written as:

$$\varepsilon = \begin{bmatrix} \varepsilon_1 & 0 & 0 \\ 0 & \varepsilon_2 & 0 \\ 0 & 0 & \varepsilon_3 \end{bmatrix} = \begin{bmatrix} \langle \varepsilon_1 \rangle & 0 & 0 \\ 0 & \langle \varepsilon_2 \rangle & 0 \\ 0 & 0 & \langle \varepsilon_3 \rangle \end{bmatrix} - \begin{bmatrix} \langle -\varepsilon_1 \rangle & 0 & 0 \\ 0 & \langle -\varepsilon_2 \rangle & 0 \\ 0 & 0 & \langle -\varepsilon_3 \rangle \end{bmatrix}$$

The equivalent strain is defined by analyzing macroscopic and microscopic analysis results that highlight the importance of the effects of tensile strain in the evolution of damage:

$$\tilde{\varepsilon} = \sqrt{\sum_{i=1}^{3} \langle \varepsilon_i \rangle_{+}^{2}} \tag{10}$$

The initial damage threshold is defined by the condition:

$$\tilde{\varepsilon} = \varepsilon_{d0} \tag{11}$$

From experimental observations carried out on cylindrical specimens, Mazars found that the micro-cracks formed during the tensile test were different from those generated by the compression stresses due to the Poisson coefficient. [7] (Fig. 7)

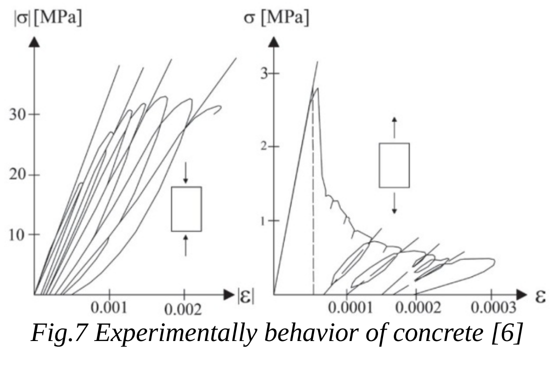

Fig.7 Experimentally behavior of concrete [6]

The activation function of the damage is defined as:

$$f(\tilde{\varepsilon}, D) = \tilde{\varepsilon} - k \tag{12}$$

where *k* represents the triggering threshold of the damage and is a variable linked to the damage triggering history [8]. The initial value associated with the first occurrence of damage can be related to the maximum tensile stress of the material indicated as σt in the following relation:

$$k_0 = \varepsilon_{d0} = \frac{\sigma_t}{E_0} \tag{13}$$

The damage triggers when the equivalent strain reaches the threshold value *k*.

Therefore, the damage variable *D* is split in two independent variables, *Dt* for tensile damage and *Dc* for the compression, in order to reproduce the behavior observed during the experimentation:

$$D = \alpha_c D_c + \alpha_t D_t \tag{14}$$

where αc αt are two variables that depending on the components of the strain.

$$\alpha_c = \sum_{i=1}^{3} \left(\frac{\langle \varepsilon_i^{-} \rangle \langle \varepsilon_i \rangle_{+}}{\tilde{\varepsilon}^2} \right)^{\beta} \tag{15}$$

$$\alpha_t = \sum_{i=1}^{3} \left(\frac{\langle \varepsilon_i^{+} \rangle \langle \varepsilon_i \rangle_{+}}{\tilde{\varepsilon}^2} \right)^{\beta} \tag{16}$$

The damage variables *Dt* and *Dc* are continuous functions while *B* is the coupling coefficient of the damage while

$$D_t = 1 - \frac{\varepsilon_{d0}(1 - A_t)}{\tilde{\varepsilon}} - \frac{A_t}{\exp\left[B_t(\tilde{\varepsilon} - \varepsilon_{d0})\right]} \tag{17}$$

$$D_c = 1 - \frac{\varepsilon_{d0}(1 - A_c)}{\tilde{\varepsilon}} - \frac{A_c}{\exp\left[B_c(\tilde{\varepsilon} - \varepsilon_{d0})\right]} \tag{18}$$

The constants *Ac*, *Bc*, *At* and *Bt* are characteristic parameters of the material and they can be obtained by calibrating the experimental results of tensile and compression tests.

The Mazars damage model has the advantage of being implemented for materials that are very close to concrete behavior, such as mortar, reducing the computational effort of numerical analysis.

Table 1 shows the values of the parameters used in order to creation the numerical model of the arch. They are partially obtained experimentally, and partially from literature.

Tab.1 Characteristic parameters of the mortar characterized by the Mazars model

Symbol	Description	Value

E_0 [N/mm^2]	Elastic modulus	700
ν_0 [-]	Poisson's ratio	0,2
k_0 [-]	Triggering threshold of damage	0,00032
A_c [-]	Shape coefficient (Compression asymptote)	1,5
B_c [-]	Shape coefficient (Compression peak)	1000
A_t [-]	Shape coefficient (Tensile asymptote)	1
B_t [-]	Shape coefficient (Tensile peak)	5000

The numerical model, by nonlinear approach, has led to the identification of different results that have validated the static test conducted on the scale model. The maximum force that generated the event in the simulation was equal to 6.26 kN, it is very close to the first cracking load experimentally obtained. Moreover, it highlights such also, in this case, the damage is developed in the same section identified during the experimental campaign, in the cross-section related to 45 ° (Fig. 8).

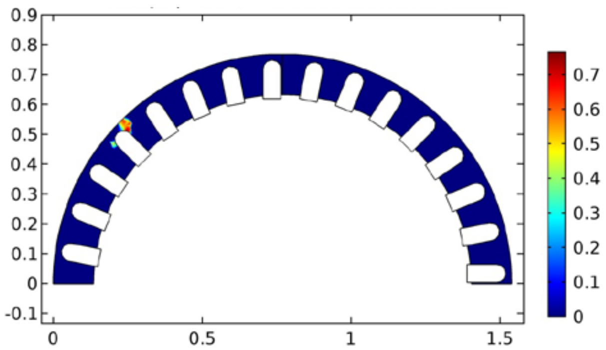

Fig.8 Development of fracture in the numerical model by Mazars Damage Model

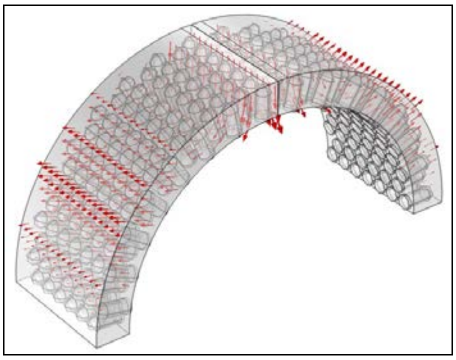

Fig.8 Distribution of tensile stress at load equal to 6,26 kN

CONCLUSIONS

The paper deals with a historical construction technique typical of the Mediterranean area and in particular of the regions of south Italy as Calabria and Puglia. This technique is characterized by the use of special hollow clay bricks called fictile tubules. For the aim of this work, experimental and numerical analyses were conducted in order to evaluate the behavior of an arch built with fictile tubule bricks.

The experimental results were validated in a first step with an analytical verification. Afterwards, a numerical model of a masonry arch was created using COMSOL to replicate the in-scale physical model. At the end, all results were compared.

REFERENCES

[1] S. Tiberti, C. Scuro, R. Codispoti, R.S. Olivito, G. Milani, “Traditional masonry arches and domes with fictile tubules in Mediterranean seismic areas: advanced numerical models and experimentation” COMPDYN 2017 6th Rhodes Island, Greece, 15–17 June 2017

[2] Olivito, R.S., Scuro, C., Codispoti, R. Experimental analysis of typical hollow clay fictile tubules of cultural heritage of Mediterranean area, Proceedings of the 10th International Conference on Structural Analysis of Historical Constructions, SAHC 2016, pp. 1362-1369.

[3] C. Scuro, S. Tiberti, R. Codispoti, R.S. Olivito, G. Milani, “On the behavior of fictile tubules masonry in Mediterranean seismic areas: application on masonry arch”, 3rd International Conference on PROHITECH Lisbon, Portugal, 12 – 15 July, 2017.

[4] Storz S., “La tecnica edilizia romana e paleocristiana delle volte e cupole a tubi fittili”, p. 28 (il saggio alle pp. 23-41) in Claudia Conforti, Lo specchio del cielo, Milano, Electa, pp. 309, 1997.

[5] Tiberti S. Scuro C. Codispoti R. Olivito R.S. Milani G., “Post-Cracking FRCM Strengthening of an Arch Composed by Hollow Clay Elements Embedded in Mortar: Experimental Investigations and Numerical Analyses”, Key Engineering Materials ISSN: 1662-9795, Vol. 747, pp 142-149, 2017.

[6] Mazars J.,“Application de la mécanique de l’endommagement au comportement non linéaire et à la rupture du béton de structure”. Thèse de Doctorat d’Etat, L.M.T., Université Paris, France, 1984.

[7]Casella V., De Sortis A., Vestroni F. (2012) Stima del danno in edifici di muratura soggetti a cedimenti Associazione Geotecnica Italiana n.1.

[8]Betti M. Bartoli G. Corazzi R. Kovacevic V. (2012) Strumenti open source per l’ingegneria strutturale modellazione meccanica non lineare di edifici in muratura. Bollettino ingegneria n. 1.